Nucleic Acids Research, 2003, Vol. 31, No. 23 ***6841–6851***
DOI: 10.1093/nar/gkg884

High mobility group A2 protein and its derivatives bind a specific region of the promoter of DNA repair gene *ERCC1* and modulate its activity

Lars Borrmann, Ralf Schwanbeck[1,*], Tomasz Heyduk[2], Birte Seebeck, Piere Rogalla, Jörn Bullerdiek and Jacek R. Wiśniewski[1]

Center for Human Genetics, University of Bremen, Leobenerstr. ZHG, D-28359 Bremen, Germany, [1]III. Zoologisches Institut-Entwicklungsbiologie, Universität Göttingen, Humboldtallee 34A, D-37073, Germany and [2]Edward A. Doisy Department of Biochemistry and Molecular Biology, St Louis University, Medical School, St Louis, MO 63104, USA

Received August 28, 2003; Revised and Accepted October 7, 2003

ABSTRACT

High mobility group A2 (HMGA2) chromosomal non-histone protein and its derivatives play an important role in development and progression of benign and malignant tumors, obesity and arteriosclerosis, although the underlying mechanisms of these conditions are poorly understood. Therefore, we tried to identify target genes for this transcriptional regulator and to provide insights in the mechanism of interaction to its target. Multiple genes have been identified by microarray experiments as being transcriptionally regulated by HMGA2. Among these we chose the *ERCC1* gene, encoding a DNA repair protein, for this study. DNA-binding studies were performed using HMGA2 and C-terminally truncated ΔHMGA2, a derivative that is frequently observed in a variety of tumors. A unique high affinity HMGA2 binding site was mapped to a specific AT-rich region located –323 to –298 upstream of the *ERCC1* transcription start site, distinguishing it from other potential AT-rich binding sites. The observed 1:1 stoichiometry for the binding of wild-type HMGA2 to this region was altered to 1:2 upon binding of truncated ΔHMGA2, causing DNA bending. Furthermore, the regulatory effect of HMGA2 was confirmed by luciferase promoter assays showing that *ERCC1* promoter activity is down-regulated by all investigated HMGA2 forms, with the most striking effect exerted by ΔHMGA2. Our results provide the first insights into how HMGA2 and its aberrant forms bind and regulate the *ERCC1* promoter.

INTRODUCTION

Nucleotide excision repair (NER) is the main pathway by which mammalian cells protect themselves from helix-distorting DNA lesions induced by UV-light and chemical mutagens (reviewed in 1). ERCC1 (excision repair cross-complementing rodent repair deficiency, complementation group 1) is one of the proteins essential for the NER pathway and is considered a marker for NER activity (2). The ERCC1 gene is located at 19q13.2–q13.3 and encodes a 32 kDa protein that is highly conserved with homologs in mouse, *mErcc1* (3), *Saccharomyces cerevisiae*, *RAD10* (4) and *Schizosaccharomyces pombe*, *swi10* (5). *In vivo*, ERCC1 forms a tight heterodimer with XPF (*syn.:* ERCC4) (6,7) that acts as a structure-specific endonuclease, cutting single-strand DNA near the junction between single- and double-stranded DNA. Within the NER pathway the ERCC1–XPF complex is responsible for the cleavage of the damaged DNA strand 16–25 nt upstream of the lesion (8–10). The repair of intrastrand and/or interstrand cross-links induced by chemotherapeutic agent cisplatin is primarily performed by the NER pathway (11–13). Furthermore, in the last few years it has been shown that the ERCC1–XPF complex is also involved in recombination events such as targeted homologous recombination (14) and targeted gene replacement (15).

HMGA2 belongs to the high mobility group (HMG) family of non-histone chromatin proteins (reviewed in 16) and its gene is located on chromosome 12q14–15 in humans. HMGA2 consists of three DNA-binding domains (AT-hooks), enabling their binding to the minor groove of AT-rich DNA, and an acidic C-tail responsible for protein–protein interactions (reviewed in 17). The DNA binding of the so called 'architectural transcription factors' HMGA were shown to alter DNA conformation and bend DNA in some cases, so that the assembly and function of transcriptional

*To whom correspondence should be addressed at present address: Tel: +1 301 594 6670; Fax: +1 301 435 3697; Email: ralf.schwanbeck@gmx.net
Present addresses:
Ralf Schwanbeck, NIH, National Cancer Institute, Building 37, Room 6060B, Bethesda, MD 20892-4255, USA
Piere Rogalla, alcedo biotech GmbH, Leobenerstrasse, ZHG, D-28359 Bremen, Germany
Jacek R. Wiśniewski, MDS Inc., Denmark, Stærmosegårdsvej 6, DK5230 Odense M, Denmark

The authors wish it to be known that, in their opinion, the first two authors should be regarded as joint First Authors

complexes is modulated resulting in regulation of gene expression. However, the available information about gene regulatory effects on a molecular level is mostly restricted to HMGA1, a related protein family (consisting of HMGA1a and HMGA1b) that is encoded from another gene and with different expression patterns and functions.

HMGA2 is expressed at very high levels during embryonic development whereas it is almost undetectable in differentiated cells (18,19). Reactivation of expression in differentiated cells is characteristic for malignant (20–23) and benign tumors (24,25) and is implicated in the formation of arteriosclerotic plaques, aortic restenosis (26) and adipogenesis (27,28). Aberrations of the chromosomal region 12q14–15 affecting the *HMGA2* gene, a frequent event in a variety of human benign tumors, is the main cause for reactivated *HMGA2* expression or the expression of chimeric or truncated forms of *HMGA2* (24,29,30). These chimeric and truncated transcripts consist predominantly of sequences encoding the three DNA-binding domains of HMGA2 but lack the acidic C-tail and its 3′UTR. For the chimeric forms of HMGA2 several fusion partner genes such as *LPP* (31), *RAD51L1* (32) and *ALDH2* (33) have been described.

Expression of both normal and truncated HMGA2 is capable of inducing neoplastic transformation *in vitro* (34). But in contrast to full-length HMGA2, transgenic mice carrying a truncated HMGA2 develop a giant phenotype along with adiposity and show an abnormally high prevalence of lipomas (35,36).

Data of cDNA expression array experiments that were performed using primary cells of three independent human myomata with normal karyotype (unpublished data) had revealed that an overexpression of HMGA2 leads to an increase in *ERCC1* transcription. As the expression of this gene is involved in the resistance of tumors to chemotherapeutic treatment we sought to identify mechanisms by which HMGA2 exerts its regulatory role on the expression of *ERCC1*. To address this question, electrophoretic mobility assays, DNA-footprinting and methylation interference assays were performed to map binding sites for HMGA2, chimeric HMGA2/LPP and C-terminally truncated ΔHMGA2 within the *ERCC1* promoter. Luminescence resonance energy transfer (LRET) measurements were used to monitor changes in DNA-bending induced by these proteins. To give insights into the functional role of these HMGA2 protein variants in terms of *ERCC1* gene regulation, *ERCC1* promoter regions were used to perform transcription assays using a luciferase reporter system.

MATERIALS AND METHODS

Preparation of the HMGA2 proteins

The proteins were expressed in *Escherichia coli* and purified as described previously (37,38). The purified products were quantified on Coomassie Blue R-stained SDS–polyacrylamide gels using a spectrophotometric determined tryptophane-containing mutant of *Chironomus* HMGA protein as a standard (39).

Construction of *ERCC1* promoter plasmids

ERCC1 promoter fragments were PCR amplified using XhoI-linker primer 5′-CCCTCGAGCTCCCCAACACTTCCAATCCTCT-3′ (nt 26426–26404; M63796) for the 3.9 kb promoter fragment (nt –3900 to +1 relative to the transcriptional start site) or BglII-linker primer 5′-AGATCTAACCGTAAGCTCCGGGAGGACAAC-3′ (nt 22952–22929) for the 426 bp promoter region (nt –425 to +1) in combination with HindIII-linker primer 5′-AAGCTTTCCGGCCTCTCTGGCCCCGC-3′ (nt 22527–22546).

Standard hotstart PCRs were performed with *Pfu* DNA polymerase (Promega, Madison, WI) in a Mastercycler gradient (Eppendorf, Hamburg, Germany) using the following protocols: 5 min 95°C, (45 s 94°C, 45 s 65°C, 4 min 72°C) 30× 10 min 72°C. Amplification of the 3.9 kb *ERCC1* fragment PCR was performed with the TripleMaster PCR system (Eppendorf) under high-fidelity PCR conditions according to the instructions of the manufacturer. PCR profile was: 3 min 94°C (20 s 94°C, 15 s 69°C, 2 min 45 s 72°C) 30× 10 min 72°C. One hundred and fifty nanograms of genomic DNA were used as templates. PCR fragments were cloned into the BglII–HindIII, respectively the XhoI–HindIII sites of reporter-gene vector pGL3-Basic (Promega).

Preparation of *ERCC1* DNA

Different fragments of the *ERCC1* promoter were cut out from the appropriate plasmids using EcoRI, and the overhanging 5′ end was filled up with Klenow fragment using [α-^{32}P]dATP. For end-labeling purposes, DNA was cut asymmetrically with SpeI resulting in a 3′-labeled top strand. All labeled inserts were purified on a 2% agarose/TBE gel. The 44 bp fragment of the *ERCC1* promoter was prepared from synthetic oligonucleotides (MWG-Biotech, Germany) comprising promoter region –330 to –287 relative to the transcription start site. For DNA footprinting experiments and mobility shift assays, the single strands were 5′ end-labeled by T4 polynucleotide kinase and complementary strands were annealed by a temperature gradient from 90 to 20°C over 2 h. The double-stranded DNA fragments were purified by ionic exchange chromatography using a Gen-Pak FAX column (Waters, 4.6 × 100 mm) with a linear gradient of 40–55% Eluent B (1 M NaCl, 1 mM EDTA, 25 mM Tris–HCl, pH 7.9) for 30 min (Eluent A: 1 mM EDTA, 25 mM Tris–HCl, pH 7.9).

Mobility shift assay

Electrophoretic mobility shift assays were carried out as described previously (40). Briefly, purified proteins were incubated with <1 nM labeled DNA in 180 mM NaCl, 1 mM $MgCl_2$, 0.01% BSA, 8% glycerol, 10 mM Tris–HCl, pH 7.9 at 20°C for 10 min. The DNA and DNA protein complexes were run on 6 or 8% polyacrylamide gels in a circulating electrophoresis buffer containing 6.6 mM Tris, 3.3 mM acetate, pH 7.9.

Hydroxyl-radical DNA footprinting

For footprints of the long DNA fragments, 16 000 c.p.m. of the *ERCC1* DNA (–426 to –257) labeled at the 3′ end of the top strand was partially digested with hydroxyl-radicals in 10 µl reaction volume in the presence or absence of 100 nM HMGA2 protein in 180 mM NaCl, 20 ng/µl BSA and 10 mM

MOPS buffer, pH 7.2 at room temperature for 20 min as described previously (41). The reaction products were separated on 8% polyacrylamide sequencing gels containing 7 M urea/TBE. For the footprints of the short DNA fragments 10–15 kc.p.m. of the 5′-labeled *ERCC1* fragment –330 to –287 was partially digested as described above. The reaction products were separated on 18% polyacrylamide sequencing gels containing 7 M urea/TBE. All gels were scanned by PhosphorImager (Molecular Dynamics) and the data analyzed as described previously (41).

Methylation interference assay

The top strand 5′-labeled –330 to –287 fragment was methylated with dimethyl sulfate (42). Five hundred nanomolar modified DNA was incubated with 1 µM HMGA2 or ΔHMGA2, and the protein–DNA complexes were separated from unbound DNA by gel electrophoresis. The DNAs out of the complexes were eluted from the gels and cleaved at methylated purines with piperidine. Finally, equal amounts of radioactivity (~5000 c.p.m.) of the cleavage products were analyzed on 18% acrylamide sequencing gels. G+A standard was generated according to Maxam and Gilbert (43). The gels were scanned and the data analyzed as described previously (41). Briefly, the peaks of the intensity plots were aligned using the program ALIGN (Dr T. Heyduk, St Louis, MO) and gel-loading efficiency was normalized. The intensities of the modified bands were integrated, and binding interference expressed as normalized difference using the following formula: $\Delta_{norm} = (I_{bound} - I_{unbound})/I_{unbound}$, where Δ_{norm} is the normalized difference, I_{bound} and $I_{unbound}$ are the integration of the normalized intensities at a single nucleotide position bound or unbound to HMGA2 (or ΔHMGA2) protein, respectively.

Luminescence resonance energy transfer (LRET) measurements

Oligonucleotides (23 nt) corresponding to *ERCC-1* promoter region from –316 to –296 were synthesized on an Applied Biosystems model 394 DNA synthesizer (Foster City, CA) using standard phosphoramidite chemistry. Oligonucleotides were purified and labeled with luminescence donor [(Eu^{3+})DTPA-AMCA-maleimide; prepared as described by Heyduk and Heyduk (44)] and fluorescence acceptor (Cy5; from Amersham Pharmacia Biotech, Piscataway, NJ) as described previously (45). The Amine-VN Phosphoramidite (Clontech, Palo Alto, CA) was used to incorporate the reactive amine into the internal positions within the oligonucleotides. LRET (46) measurements were performed at 25°C in a 120 µl cuvette on a laboratory-built two-channel instrument described earlier (47). Reaction mixtures contained 15 nM labeled DNA duplex in 10 mM Tris–HCl (pH 7.9) buffer containing 180 mM NaCl, 1 mM $MgCl_2$ and various concentrations of HMGA2 proteins. The donor emission was collected using a 620 nm interference filter (Oriel, Stratford, CT) whereas sensitized acceptor signal was detected using a 668 nm interference filter (Oriel, Stratford, CT). Sensitized acceptor (47) decay curves were analyzed by non-linear regression using SCIENTIST (Micromath Scientific Software, Salt Lake City, UT) according to:

$$I = \Sigma I_i \times \exp(-t/\tau_i) + B$$

where I_i and t_i are the amplitude and the lifetime of the ith component and B is the background noise. Energy transfer (48,49) was calculated using:

$$E = 1 - \tau_{DA}/\tau_D$$

where τ_{DA} and τ_D are luminescence lifetimes of the donor in the presence and absence of the acceptor, respectively. The distances between donor and acceptor were calculated using procedures outlined in (47) according to:

$$R^6 = R^6_o(1 - E)/E$$

where R is a distance between a donor and an acceptor, and R_o is a distance at which the energy transfer is 0.5. The R_o for (Eu^{3+})DTPA-AMCA and Cy5 donor-acceptor pair (55 Å) was calculated as described previously (50).

Luciferase promoter assays

ERCC1 promoter constructs –3900 to +1 and –425 to +1 as well as empty vector pGL3-Basic were each transiently co-transfected with a vector expressing either no HMGA2 [vector pCR3.1 (Invitrogen, Groningen, The Netherlands) as reference sample], wild-type HMGA2, C-terminally truncated HMGA2 lacking its last two exons corresponding to the spacer and acidic domain (ΔHMGA2), or chimeric HMGA2/LPP consisting of the three DNA-binding domains of HMGA2 (exons 1–3) and three LIM-domains of LPP (exons 9–11) [vectors as described elsewhere (34)]. To provide a standard for normalized vector pRL-Tk (Promega) was also co-transfected with each sample.

Transient transfections were carried out in HMGA2-negative HeLa cells being cultured in medium TC199 supplemented with 20% fetal calf serum (FCS) and antibiotics (200 IU/ml penicillin, 200 µg/ml streptomycin). Prior to transfection, cells were seeded on 6-well plates and grown to ~60% confluence. Growth medium was completely removed, cells were washed with PBS and 'transfection complexes' mixed with 800 µl culture medium were added. Transfection complexes containing 1 µg of promoter construct DNA, 1 µg of HMGA2 expression plasmid, 250 ng of pRL-TK and 10 µl of SuperFect transfection reagent (Qiagen, Hilden, Germany) were formed in a total volume of 100 µl in TC199 medium (without supplements) by incubating the sample for 10 min at room temperature according to the instructions of the manufacturer. After an incubation for 3 h, cells were washed with PBS, 2.5 ml of fresh 20% culture medium was added and cells were then grown for a further 48 h with renewal of the growth medium after 24 h.

Luciferase activities were measured in a luminometer, (Biocounter M2010, Lumac BV, The Netherlands) using the Dual-Luciferase Reporter Assay System (Promega) following the instructions of the manufacturer. Experiments for each sample were performed in duplicate and repeated several times. Data normalization and adjusting was performed as suggested by the manufacturer (Promega).

For statistical analysis, mean values of the independent experiments as well as standard deviations were calculated. To test for statistical significance one sample *t*-tests were performed with $P < 0.05$ for significant and $P < 0.01$ for highly significant differences.

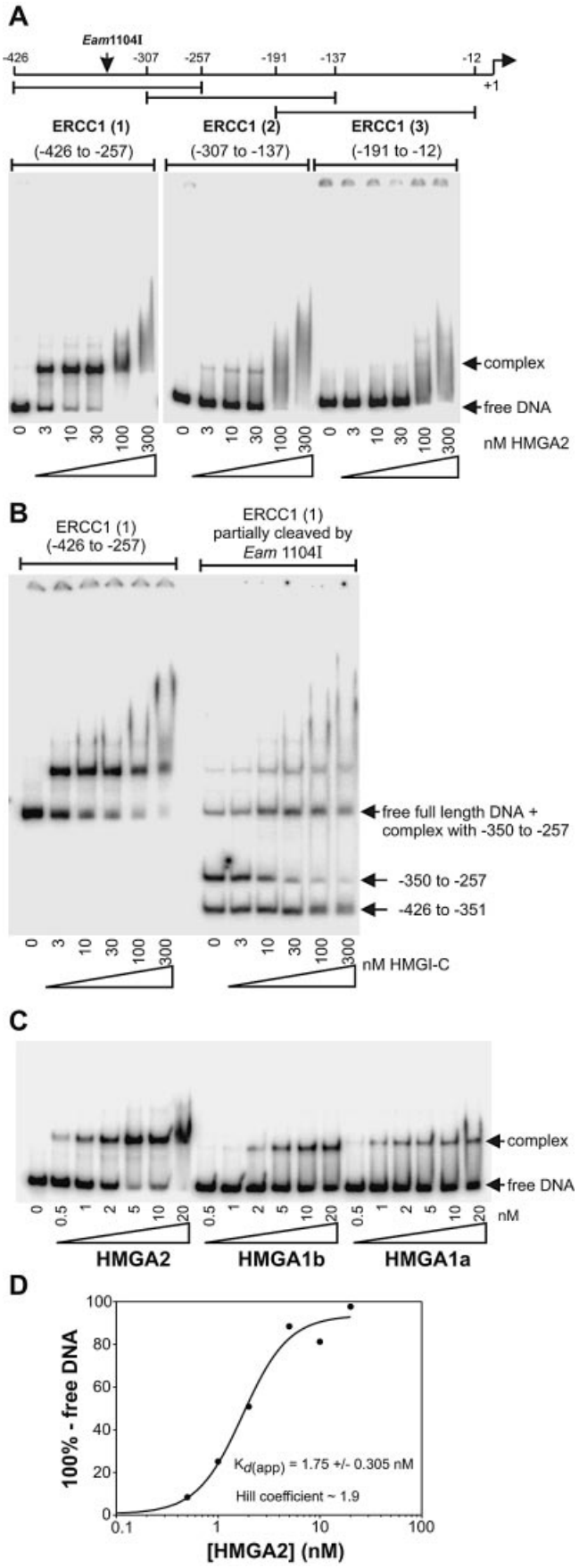

RESULTS

High affinity binding sites within the *ERCC1* promoter

DNA fragments spanning three regions of the basal *ERCC1* gene promoter (Fig. 1A, top) were ^{32}P-labeled and assayed for binding to HMGA2 protein. Mobility shift experiments revealed that HMGA2 binds tightly to the –426 to –257 fragment of the promoter whereas the other fragments showed non-specific DNA binding at higher protein concentrations without any complex formation (Fig. 1A). Digestion of this DNA fragment with a restriction enzyme into two smaller fragments showed that the –350 to –257 fragment was shifted in the presence of the protein whereas the –426 to –351 fragment did not (Fig. 1B). Note that the restriction enzyme Eam1104I does not digest its substrate completely and that the HMGA2 [–350 to –257] complex co-migrates with the full-length DNA (–426 to +1) so that the mobility shift pattern is more complex. However, the experiment clearly indicates that the –350 to –257 region contains a HMGA2 binding site.

To obtain more quantitative binding data, the mobility shift assays were repeated in a more narrow range of protein concentrations (Fig. 1C). Quantification of HMGA2 affinity to the –426 to –257 fragment revealed a $K_{d(app)}$ of 1.75 ± 0.305 nM (Fig. 1D). Hence, HMGA2 posses a fairly high affinity to this promoter region, whereas HMGA1b and HMG1b (formerly HMGY and HMGI) revealed a much lower affinity (Fig. 1C). The HMGA2 concentration needed for shifting 50% of the *ERCC1* promoter was at least one order of magnitude lower than the concentrations of HMGA1b and HMGA1a necessary to achieve the same effect. Thus, these results indicate that HMGA2 exhibits a clear specificity for a site located on this fragment.

Mapping of the HMGA2 binding site on the *ERCC1* promoter

In order to obtain detailed information on the position of the HMGA2 binding site, DNA footprinting analyses were performed. In an initial experiment the large –426 to –257 fragment labeled on the 3′ end of the top strand was analyzed. Even if the individual bands produced by the hydroxyl-radical digestion are difficult to distinguish on the plain PhosphorImage (Fig. 2A) the quantitative analysis of the digestion patterns of the free and protein-bound DNA revealed two strongly protected regions that were cut much less than the

Figure 1. Identification of the high affinity HMGA2 binding site on the *ERCC1* promoter. (**A**) Less than 1 nM ^{32}P-end-labeled fragments –426 to –257, –307 to –137 and –191 to –12 of the *ERCC1* promoter (top) were incubated with increasing concentrations of HMGA2 and electrophoresed on 6% polyacrylamide gels in low ionic strength buffer. The gels were dried, and radioactivity was scanned by a PhosphorImager. (**B**) The end-labeled –426 to –257 fragment was partially digested with the Eam1104I restriction nuclease cutting the fragment between –351 and –350. The digestion mixture was incubated with increasing concentrations of HMGA2 and analyzed as described in (A). (**C**) Comparison of the binding affinities of HMGA2, HMGA1b and HMG1a to the –426 to –257 *ERCC1* fragment using a more narrow protein concentration range as described in (A). (**D**) Quantification of the HMGA2 binding data of (C). 100% – free DNA was plotted against the protein concentration on a logarithmic scale. The line represents the theoretical curve calculated from the relationship K_d = [100% – % free DNA] × [free protein]/[complexes] using SigmaPlot Hill regression. $K_{d(app)}$ was 1.75 ± 0.31 nM for the –426 to –257 fragment.

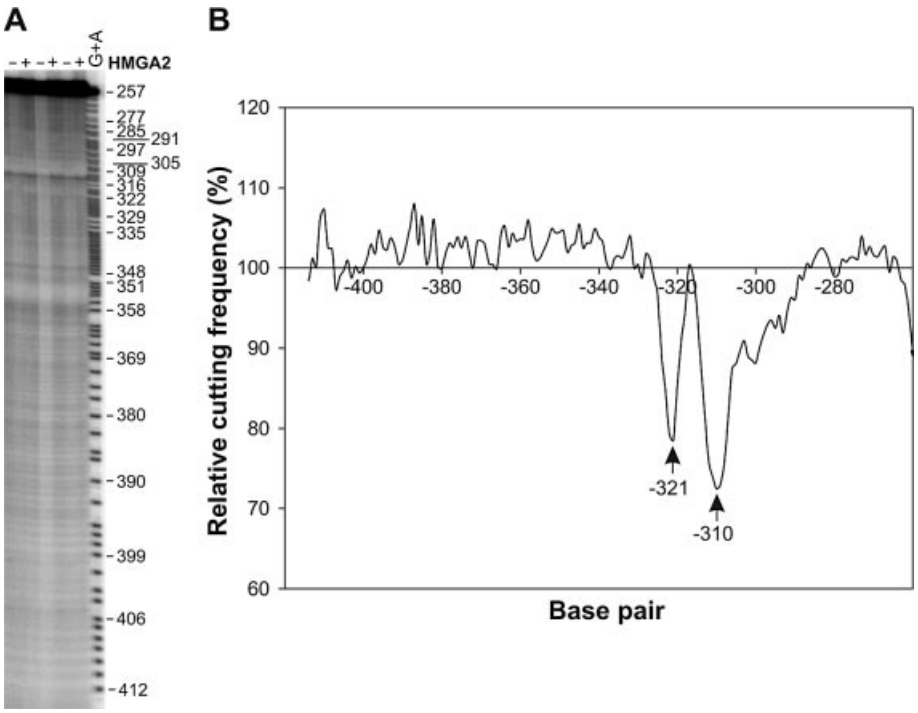

Figure 2. Footprinting of the HMGA2 on the end-labeled –426 to –257 fragment of the *ERCC1* promoter. The *ERCC1* promoter DNA that was ^{32}P end-labeled at the 3′ of the top strand was digested with hydroxyl-radicals in the absence (–) or presence (+) of 100 μM HMGA2. (**A**) reaction products were separated on 8% acrylamide sequencing gels and dried gels were scanned by PhosphorImager. A G+A standard according to Maxam and Gilbert (44) is shown in the right lane. (**B**) Quantification of the DNA footprinting data shown in (A). The 100% cutting frequency corresponds to digestion of the DNA fragment in the absence of protein so that lower values mean protection upon HMGA2 binding. Arrows label the maxima of protection. The presented results are mean values from three independent experiments.

average 100% (Fig. 2B). The maxima of these two sites were mapped to –321 and –310. More detailed quantitative DNA footprinting analysis using a 44 bp fragment comprising the nucleotides –330 to –287 showed that binding of the protein results in the protection of regions –323 to –318 and –312 to –304 on the top strand with maxima at –321 and –309, respectively. On the bottom strand the regions –314 to –305 and –303 to –298 with maxima at –310 and –301, respectively, were protected (Fig. 3A and B, black bars). The results indicate that HMGA2 binds tightly within the AT-rich minor grove spanning the region from –312 to –305. It contacts both strands in this region whereas the binding at two other sites appears to be weaker and involves just one strand.

Binding of the truncated HMGA2 to the *ERCC1* promoter

DNA footprinting experiments using the C-terminally truncated ΔHMGA2 revealed altered DNA binding properties compared to the wild-type protein (Fig. 3A and B, gray bars). When using the C-terminally truncated ΔHMGA2 the top strand central binding region around –309 was extended to the 3′ end to –301 with a second peak at –304. The bottom strand region between the protection maxima –310 and –301 was protected much more strongly than by the wild-type HMGA2. Furthermore, the truncation resulted in an additional protected region with a maximum at –295 (Fig. 3B, gray bars). In agreement with these results, mobility shift experiments using the –330 to –287 fragment with HMGA2 and ΔHMGA2 revealed clear differences in the stoichiometry of binding to the *ERCC1* promoter. Whereas the wild-type protein formed only 1:1 complexes (Fig. 4A, HMGA2), the truncated protein formed complexes with both a 1:1 and 2:1 protein to DNA ratio (Fig. 4A, ΔHMGA2). Furthermore, the slope of the binding curves with a corresponding Hill coefficient of 1.4 ± 0.2 for HMGA2 compared to 4.5 ± 0.9 for ΔHMGA2 indicates a transition from a non-cooperative to a cooperative binding upon truncation of the protein (Fig. 4B). However, the binding affinity is independent of the presence of the acidic tail. Approximately 10 nM of both proteins were necessary for shifting 50% of the 44 bp *ERCC1* DNA (Fig. 4B). For methylation interference assays both the 1:1 and the 2:1 complex visible in the mobility shift experiments (Fig. 4A) were isolated from preparative gels and compared to the single complex occurring with HMGA2. The experiments clearly demonstrated that the nature of the complexes with the 1:1 stoichiometry for the wild-type and the truncated proteins was similar (Fig. 4C and D, black and gray bars). The second molecule of ΔHMGA2 in the 2:1 complex, however, bound in a different manner 5′ from the central binding region (–309) thereby covering a much larger region than the wild-type protein (Fig. 4D, crisscrossed bars).

Binding of the truncated HMGA2 induces strong conformational perturbation of the *ERCC1* promoter

To analyze conformational changes of the *ERCC1* promoter upon binding of HMGA2, a series of duplex DNA spanning the promoter region from –316 to –294 was prepared. The duplexes were labeled at the 3′ end of the top or bottom strand

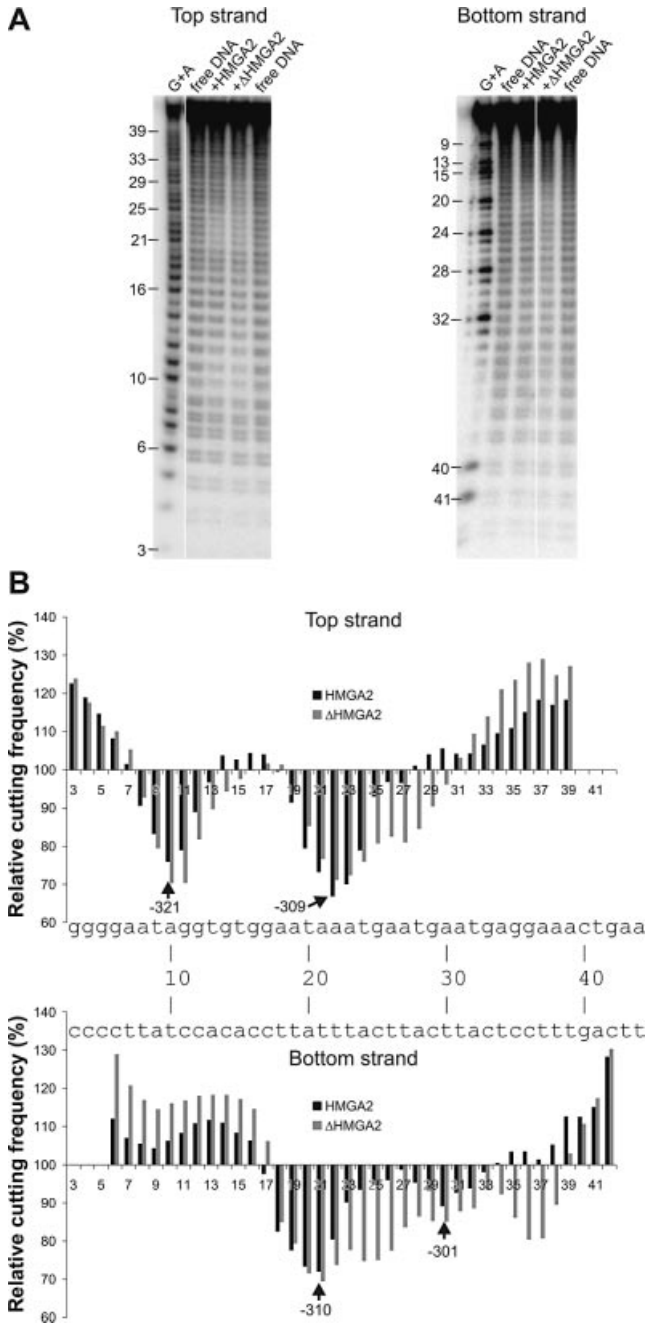

Figure 3. Fine mapping of HMGA2 (black bars) and ΔHMGA2 (gray bars) binding to the –330 to –287 region of *ERCC1* promoter fragment. (**A**) Either the top or the bottom strand was 5′ end-labeled with T4 polynucleotide kinase and the double-stranded DNA was digested with hydroxyl-radicals in the absence or presence of 100 nM of the proteins. Reaction products were separated on 18% acrylamide sequencing gels and dried gels were scanned by PhosphorImager. (**B**) Quantification of the DNA footprinting of the top strand (top) or bottom strand (bottom). Each bar shows relative cutting frequency at a single base. The 100% cutting frequency corresponds to digestion of the DNA fragment in the absence of protein so that lower values mean protection upon protein binding. The presented results are mean values from four independent experiments. The sequence of the fragment is shown between the two panels. Arrows label the maxima of protection of the wild-type protein with the corresponding nucleotide number relative to the transcription start.

with (Eu^{3+}) chelate as a donor and with Cy5 as an acceptor at three different positions within the backbone of the complementary strand. The distances between the different combinations of these fluorophores were measured by LRET for various protein concentrations (Fig. 5). The analyses revealed that ΔHMGA2 affects the DNA conformation significantly, whereas the effect of wild-type protein and the LPP-fused proteins is negligible. The effect is not a simple bending because the changes are asymmetric, i.e. the distances from one end are decreasing (Fig. 5A–C) whereas the distances from the other end (Fig. 5D–F) do not change (E) or increase (D and F). This explains why the total length between both ends remains constant in the presence of each of the proteins (data not shown). The model in Figure 6 summarizes the events that take place upon ΔHMGA2 binding.

ERCC1 promoter activity is down-regulated by different HMGA2 proteins

To investigate the effects that HMGA2 exerts on *ERCC1* transcriptional activity, a basal promoter fragment of *ERCC1* spanning region nt –425 to +1 and a 3.9 kb promoter fragment (spanning nt –3900 to +1) were cloned into reporter vector pGL3-Basic. Luciferase reporter gene assays were used to measure promoter activity of these constructs using HMGA2-negative HeLa cells for transient transfection. Both promoter constructs were co-transfected with constructs expressing either normal HMGA2, C-terminally truncated ΔHMGA2, a HMGA2/LPP fusion protein or no protein (vector pCR3.1) (Fig. 7).

Co-transfection experiments of the two ERCC1 promoter fragments with different HMGA2 protein variants showed decreased ERCC1 promoter activity due to HMGA2 proteins in all samples tested relatively to promoter constructs co-transfected with empty vector pCR3.1 expressing no HMGA2 (Fig. 7). Whereas the decrease in *ERCC1* promoter activity induced by wild-type HMGA2 was ~15% for both promoter constructs, the co-expression of truncated ΔHMGA2 decreased promoter activity to ~63%. In contrast to that, only minor changes in *ERCC1* promoter activities were observed for co-transfections with HMGA2/LPP. These promoter data are statistically significant ($P = 0.039$, 3.9 kb promoter; $P = 0.010$ basal promoter) for co-transfection experiments with wild-type HMGA2 and highly significant ($P = 0.003039$; $P = 2.9 \times 10^{-8}$) for C-terminally truncated ΔHMGA2.

As revealed by these experiments, the basal 426 bp *ERCC1* fragment had a 1.3-fold higher promoter activity with respect to the 3.9 kb fragment (data not shown) suggesting negative regulatory elements within the 3.5 kb 5′ of the basal *ERCC1* promoter fragment.

DISCUSSION

Although HMGA2 as well as its aberrant forms are thought to be implicated in the pathogenesis of benign mesenchymal tumors showing rearrangements of chromosomal region 12q14–15 (24), the exact mechanisms by which these proteins contribute to tumorigenesis are still unknown. It remains unclear why wild-type proteins of the HMGA family as well as their derivatives are similarly associated with the same tumor entities. Based on the results of cDNA expression array experiments we selected, herein, the *ERCC1* gene to analyze

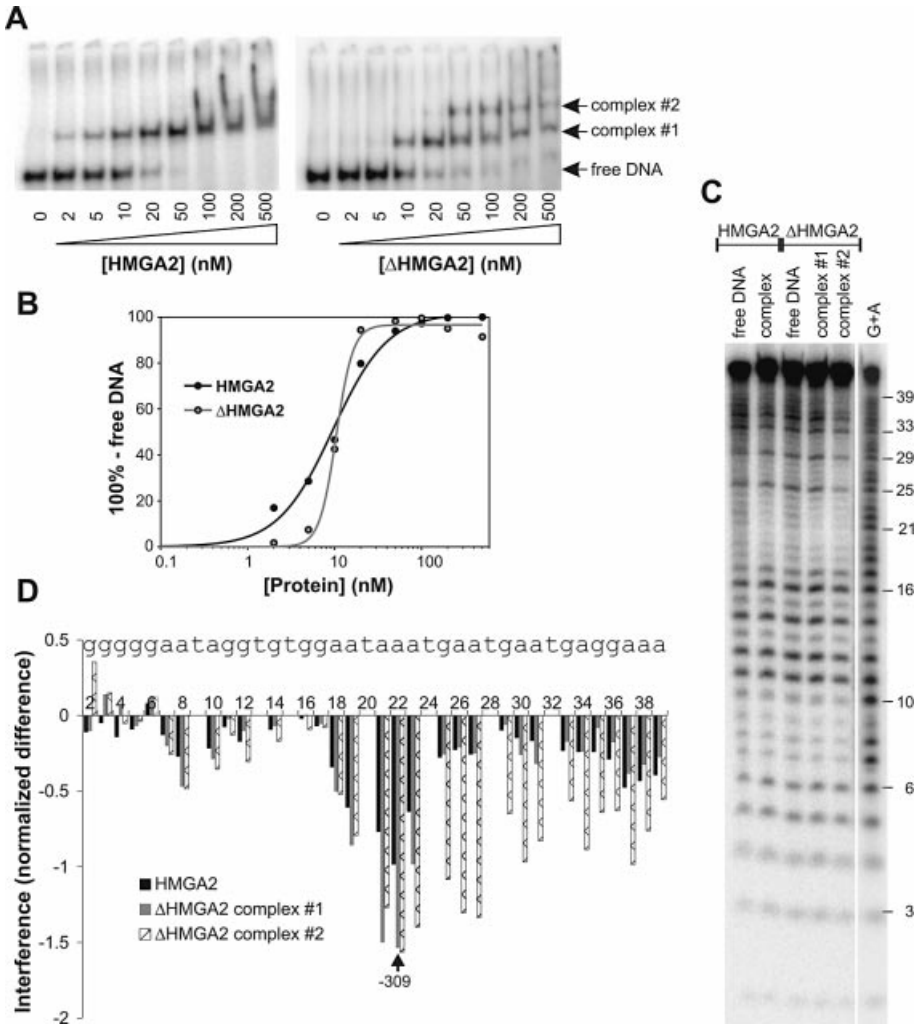

Figure 4. Truncation of the HMGA2 affects protein binding to *ERCC1* promoter. (**A**) Electrophoretic mobility shift assay. Less than 1 nM of the ^{32}P-end-labeled –330 to –287 *ERCC1* fragment was incubated with increasing concentrations of HMGA2 and ΔHMGA2 and subjected to electrophoresis on 8% polyacrylamide gels in low ionic strength buffer. The gels were dried and the radioactivity was scanned by PhosphorImager. In addition to the 1:1 complex (complex #1) a second complex is visible with ΔHMGA2 (complex #2) probably reflecting two protein molecules binding to the DNA fragment. (**B**) Quantification of the EMSA data of (A) using ImageQuant software and SigmaPlot Hill regression (see Fig. 1D). (**C**) Methylation interference assay. The –330 to –287 fragment labeled at the 5′ of the top strand was methylated with dimethyl sulfate. Five hundred nanomolar modified double-stranded DNA was incubated with 1 μM HMGA2 or ΔHMGA2, and the protein–DNA complexes were separated from unbound DNA by gel electrophoresis as shown in (A), Δ*HMGA2*. The DNA out of the complexes was eluted from the gels and cleaved at methylated purines with piperidine. Finally, equal amounts of radioactivity (~5000 c.p.m.) of the cleavage products were analyzed on 18% acrylamide sequencing gels. (**D**) Quantitative analysis of the methylation interference experiment of (C). The gels were scanned and the data analyzed as described in Materials and Methods. Negative values indicate binding interference upon the methylation of the corresponding nucleotide. Black, gray and crisscrossed bars refer to protein to DNA complexes 1:1 of HMGA2, 1:1 of ΔHMGA2 and 2:1 of ΔHMGA2, respectively. The arrow indicates the maximum of interference of the central binding site and the corresponding number represents the distance relative to the transcription start.

the mechanism of interaction of wild-type HMGA2 and its derivatives to target DNA.

We were able to map a high affinity HMGA2 binding site to an AT-rich region located –323 to –298 bp upstream of the *ERCC1* transcription start site. Despite their structural similarities, results presented herein demonstrated clearly that HMGA2 protein has at least one order of magnitude higher affinity to this *ERCC1* promoter region than both of the HMGA1 proteins (HMGA1a and HMGA1b). These data are consistent with studies comparing DNA binding properties of various HMGA proteins showing that HMGA1 and HMGA2 might interact differently with the same DNA fragment (38). For example, HMGA1 contacts the *IFN*β promoter using three AT-hooks, whereas binding of HMGA2 protein involves only two AT-hooks resulting in an ~8-fold lower affinity than HMGA1a and an ~2-fold lower affinity than HMGA1b to the *IFN*β promoter (38,41). Moreover, comparison of the binding pattern of HMGA2 with the *IFN*β promoter (41) and the *ERCC1* promoter (this work) reveals that the same protein interacts differently with distinct DNA templates. Thus, our biochemical data strongly suggest that the *ERCC1* promoter harbors an HMGA2-specific binding site.

Despite the opinion that the HMGA proteins bind non-specifically to stretches of AT-rich DNA we showed that this

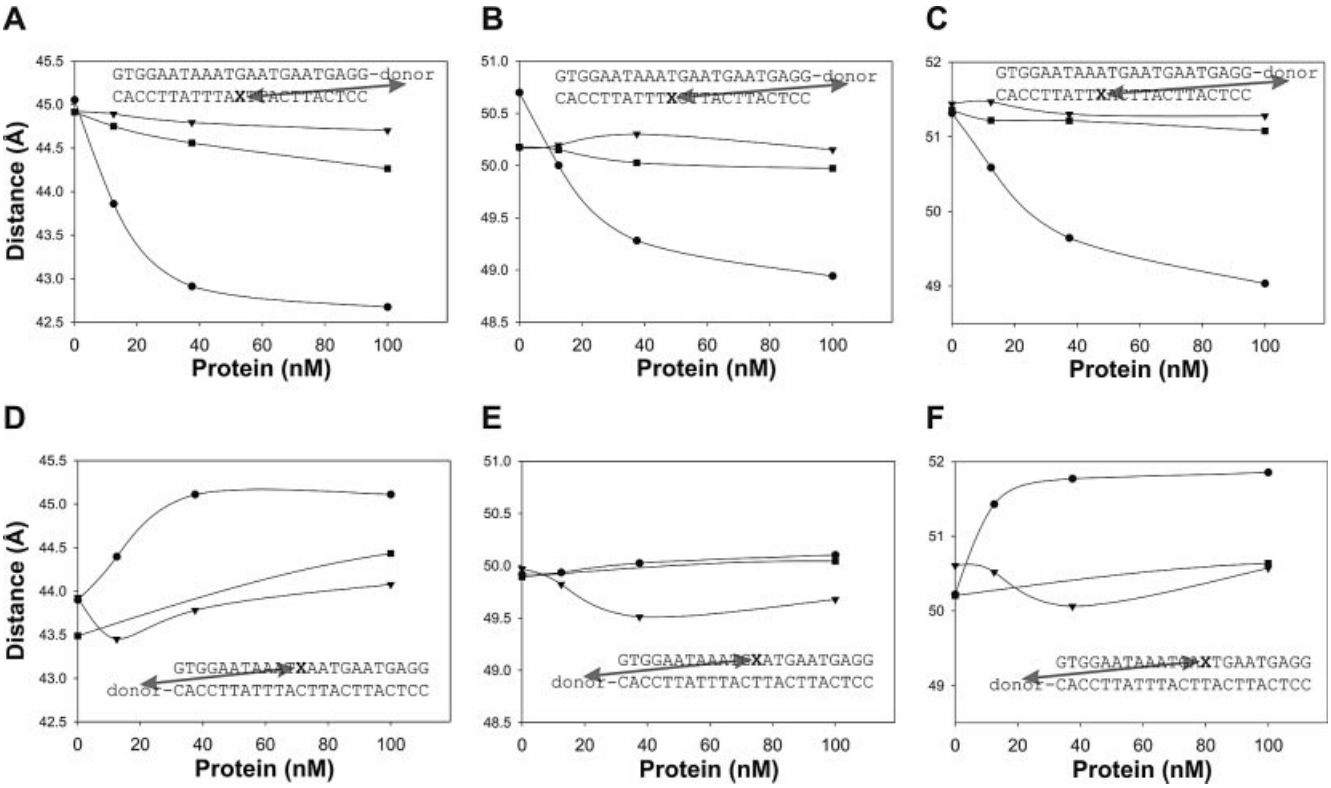

Figure 5. Perturbation of DNA *ERCC1* promoter conformation by HMGA2 and its mutants. A series of DNA constructs comprising promoter region –316 to –294 were produced either with inserted luminescence donor [(Eu3+)DTPA-AMCA-maleimide at the 3′ of the top strand (**A**–**C**) or at the bottom strand (**D**–**F**) and the fluorescence acceptor (*X*) Cy5 at different positions within the complementary strand, respectively. The LRET measurements were performed in the absence or presence of 12.5, 37 and 100 nM of HMGA2 (triangles), ΔHMGA2 (circles) and HMG2/LPP (squares). The concentration of labeled duplex was 15 nM.

property alone is not sufficient. Even AT-stretches that are spaced in the appropriate distance (10–11 bp from center to center) and would represent potential HMGA binding sites might be in fact not bound by the protein (this work and R.Schwanbeck, unpublished results). However, the presented *ERCC1* promoter site seems to be one of these gene regions specifically bound by HMGA2. Unlike the sequence-specific binding of transcription factors, the actual binding of architectural transcription factors like the HMGA proteins to certain DNA sequences is difficult to predict, and a generally valid algorithm has to be found for HMGA2, HMGA1a and HMGA1b DNA.

Binding studies for truncated ΔHMGA2 revealed that the derivative form of HMGA2 covers an extended region on the *ERCC1* promoter with the bottom strand region being much more strongly protected than by wild-type HMGA2. Clear differences were also observed for the stoichiometry of binding to the *ERCC1* promoter. Whereas the wild-type protein formed only 1:1 complexes, truncated protein formed complexes with both a 1:1 and 2:1 protein to DNA ratio with a transition from a non-cooperative to a cooperative binding upon truncation of the protein. Although the nature of the complexes with the 1:1 stoichiometry for the wild-type and the truncated proteins were similar, the second ΔHMGA2 molecule binds in a different manner covering a much larger region than the wild-type protein having a significant effect on DNA conformation. However, the affinity of binding was found to be independent of the presence of the acidic tail. The results presented herein confirmed the data described by Noro *et al.* (51) showing that the acidic C-tail is not involved in determining the specificity of HMGA2 DNA-binding in the case of a high affinity HMGA binding site. In contrast, differences in protein–DNA complexes were observed for low affinity binding sites upon C-terminal truncation of HMGA2 resulting in high molecular weight protein–DNA complexes similar to the 2:1 ΔHMGA2–DNA complexes described herein.

These differences in behavior of truncated ΔHMGA2 upon binding to the *ERCC1* promoter relative to wild-type protein were also seen for the luciferase promoter assays. Whereas luciferase assays showed that the activity of the *ERCC1* promoter is down-regulated by various HMGA2 proteins, the most striking effect was exerted by the truncated ΔHMGA2. The differences in DNA-binding stoichiometry between normal and truncated HMGA2 correlate well with their different capabilities of repressing *ERCC1* promoter activity as measured by luciferase promoter assays. Comparison of microarray experiments performed with different cell types clearly showed that gene-regulatory effects exerted by HMGA proteins depend on the cellular context in which these proteins are expressed (L.Borrmann and J.Bullerdiek, unpublished results). This variation could be the reason why the *ERCC1* promoter was found to be up-regulated within myomata cells and down-regulated by HMGA2 protein in HeLa cells, and

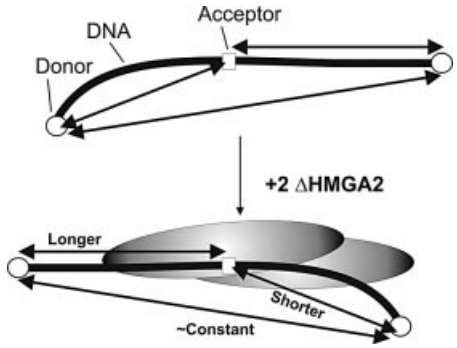

Figure 6. Model of the ΔHMGA2-induced conformational changes on the *ERCC1* promoter according to the EMSA and LRET experiments in Figures 4 and 5. The promoter region contains a prebent element (left side). Upon binding of two molecules ΔHMGA2 this prebending is reversed and on the other end of the promoter a DNA bend is introduced.

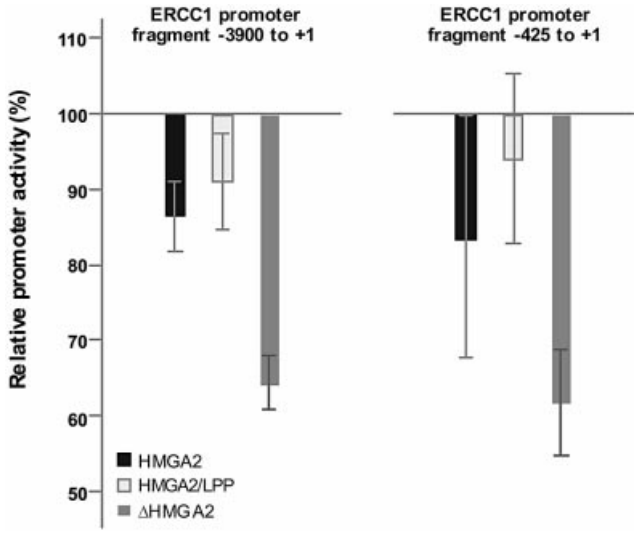

Figure 7. Activity of the *ERCC1* promoter is affected by HMGA2, HMGA2/LPP and ΔHMGA2. *ERCC1* promoter fragments –3900 to +1 and –425 to +1 relative to the transcriptional start site were cloned in luciferase reporter-gene vector pGL3-Basic. These promoter constructs were transiently co-transfected with a vector expressing either no HMGA2 (reference vector), wild-type HMGA2, chimeric HMGA2/LPP or C-terminally truncated ΔHMGA2 and vector pRL-Tk were used for normalization. Results are the mean value of several independent experiments performed within HeLa cells. The change in promoter activity of the 3.9 kb and 426 bp *ERCC1* promoter fragments in dependence of different HMGA2 protein variants are shown relative to the data obtained for the corresponding ERCC1 construct co-transfected with the reference vector. Black, white and gray bars refer to co-transfection with wild-type HMGA2, chimeric HMGA2/LPP and truncated ΔHMG2, respectively.

might also explain why HMGA1 overexpression is characteristic for malignant tumors increasing their rate of proliferation (52,53). Whereas in the context of normal cells, HMGA1 reduces rate of proliferation (54) and leads to a delayed G2-M-transition (55). However, taking into account that HMGA proteins are not able to initiate transcription per se (56), it seems reasonable, given that different cell types contain different sets of transcription factors, that the interaction of these transcription factors with HMGA-bent DNA can regulate gene expression negatively or positively depending on the cellular environment. Furthermore, higher-order chromatin structure may also play a role in the gene-regulatory effect as well as the post-translational modifications of HMGA2 that may control its activity and can be different in various cell lines.

In contrast to HMG box proteins that introduce sharp kinks into the DNA, the alterations induced by HMGA proteins are rather subtle (57) employing a reversal of intrinsically bent DNA. These slight changes, which can be crucial to form a stereospecific three-dimensional multiprotein complex, are difficult to monitor. FRET or LRET analysis can be very sensitive tools to observe these slight changes in DNA bending as we demonstrated previously (38,58). We show in this work that the ΔHMGA2 protein is also able to alter the DNA conformation within the *ERCC1* promoter, probably by the additional DNA contacts in the region –310 and –301 compared to the wild-type protein. Thus, it can be anticipated that binding of more than one ΔHMGA2 protein changes DNA conformation within the element to an extent affecting binding of transcription factors constituting potential *ERCC1* enhanceosomes.

The *ERCC1* gene, which does not contain classical promoter elements like TATA or GC boxes (59), can possibly be down-regulated by HMGA2 and its aberrant forms by modulating the chromatin structure, thus making the assembly and function of transcriptional complexes more difficult. A target of this environmental change could be the AP1 site, located 48 bp upstream of the HMGA2 binding site. Furthermore, a comparative displacement of transcription factors by HMGA2 or their interactions can also be relevant in terms of gene expression. Sequence analysis of the HMGA2 binding site revealed putative binding sites for the transcription factors Pit-1a, TEC1, Elf-1, C/EBP, ICSBP and ISGF-3. For the proteins Elf-1 and C/EBP, physical interactions with HMGA1, another member of the HMGA family, have already been described (60,54). In further studies, composition and assembly of the *ERCC1* enhanceosome upon intact and mutated HMGA2 proteins need to be examined.

In terms of the mechanisms by which HMGA proteins contribute to tumorigenesis, a reactivated expression of either HMGA2 or its derivative forms as observed within several benign mesenchymal tumor entities (24) can affect the expression of DNA-repair gene *ERCC1* leading to an altered genomic stability.

ACKNOWLEDGEMENTS

We thank Dr Ryan Ranallo (Walter Reed Army Institute of Research, Silver Spring, MD) and Dr Lori Pile (National Cancer Institute, Bethesda, MD) for critically reading the manuscript. This work was supported by the Deutsche Forschungsgemeinschaft (grant WI-1210/3-1).

REFERENCES

1. Araujo,S.J. and Wood,R.D. (1999) Protein complexes in nucleotide excision repair. *Mutat. Res.*, **435**, 23–33.
2. Westerveld,A., Hoeijmakers,J.H., van Duin,M., de Wit,J., Odijk,H., Pastink,A., Wood,R.D. and Bootsma,D. (1984) Molecular cloning of a human DNA repair gene. *Nature*, **310**, 425–429.

3. Selfridge,J., Pow,A.M., McWhir,J., Magin,T.M. and Melton,D.W. (1992) Gene targeting using a mouse HPRT minigene/HPRT-deficient embryonic stem cell system: inactivation of the mouse ERCC-1 gene. *Somat. Cell Mol. Genet.*, **18**, 325–336.
4. vanDuin,M., de Wit,J., Odijk,H., Westerveld,A., Yasui,A., Koken,H.M., Hoeijmakers,J.H. and Bootsma,D. (1986) Molecular characterization of the human excision repair gene ERCC-1: cDNA cloning and amino acid homology with the yeast DNA repair gene RAD10. *Cell*, **44**, 913–923.
5. Rodel,C., Kirchhoff,S. and Schmidt,H. (1992) The protein sequence and some intron positions are conserved between the switching gene swi10 of *Schizosaccharomyces pombe* and the human excision repair gene ERCC1. *Nucleic Acids Res.*, **20**, 6347–6353.
6. Biggerstaff,M., Szymkowski,D.E. and Wood,R.D. (1993) Co-correction of the ERCC1, ERCC4 and xeroderma pigmentosum group F DNA repair defects *in vitro*. *EMBO J.*, **12**, 3685–3692.
7. vanVuuren,A.J., Appeldoorn,E., Odijk,H., Yasui,A., Jaspers,N.G., Bootsma,D. and Hoeijmakers,J.H. (1993) Evidence for a repair enzyme complex involving ERCC1 and complementing activities of ERCC4, ERCC11 and xeroderma pigmentosum group F. *EMBO J.*, **12**, 3693–3701.
8. Mu,D., Park,C.H., Matsunaga,T., Hsu,D.S., Reardon,J.T. and Sancar,A. (1995) Reconstitution of human DNA repair excision nuclease in a highly defined system. *J. Biol. Chem.*, **270**, 2415–2418.
9. Matsunaga,T., Mu,D., Park,C.H., Reardon,J.T. and Sancar,A. (1995) Human DNA repair excision nuclease. Analysis of the roles of the subunits involved in dual incisions by using anti-XPG and anti-ERCC1 antibodies. *J. Biol. Chem.*, **270**, 20862–20869.
10. Sijbers,A.M., de Laat,W.L., Ariza,R.R., Biggerstaff,M., Wei,Y.F., Moggs,J.G., Carter,K.C., Shell,B.K., Evans,E., de Jong,M.C., Rademakers,S., de Rooij,J., Jaspers,N.G., Hoeijmakers,J.H. and Wood,R.D. (1996) Xeroderma pigmentosum group F caused by a defect in a structure-specific DNA repair endonuclease. *Cell*, **86**, 811–822.
11. Jones,J.C., Zhen,W.P., Reed,E., Parker,R.J., Sancar,A. and Bohr,V.A. (1991) Gene-specific formation and repair of cisplatin intrastrand adducts and interstrand cross-links in Chinese hamster ovary cells. *J. Biol. Chem.*, **266**, 7101–7107.
12. Zhen,W., Link,C.J., O'Connor,P.M., Reed,E., Parker,R., Howell,S.B. and Bohr,V.A. (1992) Increased gene-specific repair of cisplatin interstrand cross-links in cisplatin-resistant human ovarian cancer cell lines. *Mol. Cell. Biol.*, **12**, 3689–3698.
13. Moggs,J.G., Yarema,K.J., Essigmann,J.M. and Wood,R.D. (1996) Analysis of incision sites produced by human cell extracts and purified proteins during nucleotide excision repair of a 1,3-intrastrand d(GpTpG)-cisplatin adduct. *J. Biol. Chem.*, **271**, 7177–7186.
14. Adair,G.M., Rolig,R.L., Moore-Faver,D., Zabelshansky,M., Wilson,J.H. and Nairn,R.S. (2000) Role of ERCC1 in removal of long non-homologous tails during targeted homologous recombination. *EMBO J.*, **19**, 5552–5561.
15. Niedernhofer,L.J., Essers,J., Weeda,G., Beverloo,B., de Wit,J., Muijtjens,M., Odijk,H., Hoeijmakers,J.H. and Kanaar,R. (2001) The structure-specific endonuclease Ercc1-Xpf is required for targeted gene replacement in embryonic stem cells. *EMBO J.*, **20**, 6540–6549.
16. Reeves,R. (2001) Molecular biology of HMGA proteins: hubs of nuclear function. *Gene*, **277**, 63–81.
17. Wiśniewski,J.R. and Schwanbeck,R. (2000) High mobility group I/Y: multifunctional chromosomal proteins causally involved in tumor progression and malignant transformation (review). *Int. J. Mol. Med.*, **6**, 409–419.
18. Chiappetta,G., Avantaggiato,V., Visconti,R., Fedele,M., Battista,S., Trapasso,F., Merciai,B.M., Fidanza,V., Giancotti,V., Santoro,M., Simeone,A. and Fusco,A. (1996) High level expression of the HMGI (Y) gene during embryonic development. *Oncogene*, **13**, 2439–2446.
19. Rogalla,P., Drechsler,K., Frey,G., Hennig,Y., Helmke,B., Bonk,U. and Bullerdiek,J. (1996) HMGI-C expression patterns in human tissues. Implications for the genesis of frequent mesenchymal tumors. *Am. J. Pathol.*, **149**, 775–779.
20. Giancotti,V., Buratti,E., Perissin,L., Zorzet,S., Balmain,A., Portella,G., Fusco,A. and Goodwin,G.H. (1989) Analysis of the HMGI nuclear proteins in mouse neoplastic cells induced by different procedures. *Exp. Cell Res.*, **184**, 538–545.
21. Manfioletti,G., Giancotti,V., Bandiera,A., Buratti,E., Sautiere,P., Cary,P., Crane-Robinson,C., Coles,B. and Goodwin,G.H. (1991) cDNA cloning of the HMGI-C phosphoprotein, a nuclear protein associated with neoplastic and undifferentiated phenotypes. *Nucleic Acids Res.*, **19**, 6793–6797.
22. Tamimi,Y., van der Poel,H.G., Karthaus,H.F., Debruyne,F.M. and Schalken,J.A. (1996) A retrospective study of high mobility group protein I(Y) as progression marker for prostate cancer determined by in situ hybridization. *Br. J. Cancer*, **74**, 573–578.
23. Rogalla,P., Drechsler,K., Schröder-Babo,W., Eberhardt,K. and Bullerdiek,J. (1998) HMGIC expression patterns in non-small lung cancer and surrounding tissue. *Anticancer Res.*, **18**, 3327–3330.
24. Schoenmakers,E.F., Wanschura,S., Mols,R., Bullerdiek,J., Van den Berghe,H. and Van de Ven,W.J. (1995) Recurrent rearrangements in the high mobility group protein gene, HMGI-C, in benign mesenchymal tumours. *Nature Genet.*, **10**, 436–444.
25. Kazmierczak,B., Wanschura,S., Rommel,B., Bartnitzke,S. and Bullerdiek,J. (1996) Ten pulmonary chondroid hamartomas with chromosome 6p21 breakpoints within the HMG-I(Y) gene or its immediate surroundings. *J. Natl Cancer Inst.*, **88**, 1234–1236.
26. Chin,M.T., Pellacani,A., Hsieh,C.M., Lin,S.S., Jain,M.K., Patel,A. and Huggins,G.S. (1999) Induction of high mobility group I architectural transcription factors in proliferating vascular smooth muscle *in vivo* and *in vitro*. *J. Mol. Cell. Cardiol.*, **31**, 2199–2205.
27. Zhou,X., Benson,K.F., Ashar,H.R. and Chada,K. (1995) Mutation responsible for the mouse pygmy phenotype in the developmentally regulated factor HMGI-C. *Nature*, **376**, 771–774.
28. Anand,A. and Chada,K. (2000) *In vivo* modulation of Hmgic reduces obesity. *Nature Genet.*, **24**, 377–380.
29. Geurts,J.M., Schoenmakers,E.F. and Van de Ven,W.J. (1997) Molecular characterization of a complex chromosomal rearrangement in a pleomorphic salivary gland adenoma involving the 3′-UTR of HMGIC. *Cancer Genet. Cytogenet.*, **95**, 198–205.
30. Klotzbücher,M., Wasserfall,A. and Fuhrmann,U. (1999) Misexpression of wild-type and truncated isoforms of the high-mobility group I proteins HMGI-C and HMGI(Y) in uterine leiomyomas. *Am. J. Pathol.*, **155**, 1535–1542.
31. Petit,M.M., Mols,R., Schoenmakers,E.F., Mandahl,N. and Van de Ven,W.J. (1996) LPP, the preferred fusion partner gene of HMGIC in lipomas, is a novel member of the LIM protein gene family. *Genomics*, **36**, 118–129.
32. Schoenmakers,E.F., Huysmann,C. and Van de Ven,W.J. (1999) Allelic knockout of novel splice variants of human recombination repair gene RAD51B in t(12;14) uterine leiomyomas. *Cancer Res.*, **59**, 19–23.
33. Kazmierczak,B., Hennig,Y., Wanschura,S., Rogalla,P., Bartnitzke,S., Van de Ven,W. and Bullerdiek,J. (1995) Description of a novel fusion transcript between HMGI-C, a gene encoding for a member of the high mobility group proteins and the mitochondrial aldehyde dehydrogenase gene. *Cancer Res.*, **55**, 6038–6039.
34. Fedele,M., Berlingieri,M.T., Scala,S., Chiariotti,L., Viglietto,G., Rippel,V., Bullerdiek,J., Santoro,M. and Fusco,A. (1998) Truncated and chimeric HMGI-C genes induce neoplastic transformation of NIH3T3 murine fibroblasts. *Oncogene*, **17**, 413–418.
35. Battista,S., Fidanza,V., Fedele,M., Klein-Szanto,A.J., Outwater,E., Brunner,H., Santoro,M., Croce,C.M. and Fusco,A. (1999) The expression of a truncated HMGI-C gene induces gigantism associated with lipomatosis. *Cancer Res.*, **59**, 4793–4797.
36. Arlotta,P., Tai,A.K., Manfioletti,G., Clifford,C., Jay,G. and Ono,S.J. (2000) Transgenic mice expressing a truncated form of the high mobility group I-C protein develop adiposity and an abnormally high prevalence of lipomas. *J. Biol. Chem.*, **275**, 14394–14400.
37. Wiśniewski,J.R. and Schulze,E. (1994) High affinity interaction of dipteran high mobility group (HMG) proteins 1 with DNA is modulated by COOH-terminal regions flanking the HMG box domain. *J. Biol. Chem.*, **269**, 10713–10719.
38. Piekiełko,A., Drung,A., Rogalla,P., Schwanbeck,R., Heyduk,T., Gerharz,M., Bullerdiek,J. and Wiśniewski,J.R. (2001) Distinct organization of DNA complexes of various HMGI/Y family proteins and their modulation upon mitotic phosphorylation. *J. Biol. Chem.*, **276**, 1984–1992.
39. Schwanbeck,R., Gymnopoulos,M., Petry,I., Piekiełko,A.I., Szewczuk,Z., Zechel,K. and Wiśniewski,J.R. (2001) Consecutive steps of phosphorylation affect conformation and DNA binding of the chironomus high mobility group A protein. *J. Biol. Chem.*, **276**, 26012–26021.
40. Wiśniewski,J.R., Heßler,K., Claus,P. and Zechel,K. (1997) Structural and functional consequences of mutations within the hydrophobic cores of

the HMG1-box domain of the Chironomus high-mobility-group protein 1a. *Eur. J. Biochem.*, **243**, 151–159.
41. Schwanbeck,R., Manfioletti,G. and Wiśniewski,J.R. (2000) Architecture of high mobility group protein I-C.DNA complex and its perturbation upon phosphorylation by Cdc2 kinase. *J. Biol. Chem.*, **275**, 1793–1801.
42. Siebenlist,U. and Gilbert,W. (1980) Contacts between *Escherichia coli* RNA polymerase and an early promoter of phage T7. *Proc. Natl Acad. Sci. USA*, **77**, 122–126.
43. Maxam,A. and Gilbert,W. (1980) Sequencing end-labeled DNA with base-specific chemical cleavages. *Methods Enzymol.*, **65**, 499–525.
44. Heyduk,E. and Heyduk,T. (1999) Architecture of a complex between the sigma70 subunit of *Escherichia coli* RNA polymerase and the nontemplate strand oligonucleotide. Luminescence resonance energy transfer study. *J. Biol. Chem.*, **274**, 3315–3322.
45. Heyduk,E. and Heyduk,T. (2002) Conformation of fork junction DNA in a complex with *Escherichia coli* RNA polymerase. *Biochemistry*, **41**, 2876–2883.
46. Selvin,P.R. and Hearst,J.E. (1994) Luminescence energy transfer using a terbium chelate: improvements on fluorescence energy transfer. *Proc. Natl Acad. Sci. USA*, **91**, 10024–10028.
47. Heyduk,E. and Heyduk,T. (2001) Luminescence energy transfer with lanthanide chelates: interpretation of sensitized acceptor decay amplitudes. *Anal. Biochem.*, **289**, 60–67.
48. Förster,T. (1948) Intermolecular energy migration and fluorescence. *Ann. Phys.* (Leipzig), **2**, 55–77.
49. Lakowicz,J.R. (1999) Principles of Fluorescence Spectroscopy, Kluwer Academic/Plenum Press, New York, NY.
50. Heyduk,E. and Heyduk,T. (1997) Thiol-reactive, luminescent Europium chelates: luminescence probes for resonance energy transfer distance measurements in biomolecules. *Anal. Biochem.*, **248**, 216–227.
51. Noro,B., Licheri,B., Sgarra,R., Rustighi,A., Tessari,M.A., Chau,K.Y., Ono,S.J., Giancotti,V. and Manfioletti,G. (2003) Molecular dissection of the architectural transcription factor HMGA2. *Biochemistry*, **42**, 4569–4577.
52. Giancotti,V., Pani,B., D'Andrea,P., Berlingieri,M.T., DiFiore,P.P., Fusco,A., Veccio,G., Philip,R., Crane-Robinson,C., Nicolas,R.H., Wright,C.A. and Goodwin,G.H. (1987) Elevated levels of a specific class of nuclear phosphoproteins in cells transformed with v-ras and v-mos oncogenes and by cotransfection with c-myc and polyoma middle T genes. *EMBO J.*, **6**, 1981–1987.
53. Reeves,R., Edberg,D.D. and Li,Y. (2001) Architectural transcription factor HMGI(Y) promotes tumor progression and mesenchymal transition of human epithelial cells. *Mol. Cell. Biol.*, **21**, 575–594.
54. Melillo,R.M., Pierantoni,G.M., Scala,S., Battista,S., Fedele,M., Stella,A., De Biasio,M.C., Chiappetta,G., Fidanza,V., Condorelli,G., Santoro,M., Croce,C.M., Viglietto,G. and Fusco,A. (2001) Critical role of the HMGI(Y) proteins in adipocytic cell growth and differentiation. *Mol. Cell. Biol.* **21**, 2485–2495.
55. Fedele,M., Pierantoni,G.M,, Berlingieri,M.T., Battista,S., Baldassarre,G., Munshi,N., Dentice,M., Thanos,D., Santoro,M., Viglietto,G. and Fusco,A. (2001) Overexpression of proteins HMGA1 induces cell cycle deregulation and apoptosis in normal rat thyroid cells. *Cancer Res.*, **61**, 4583–4590.
56. Thanos,D. and Maniatis,T. (1992) The high mobility group protein HMG I(Y) is required for NF-κB-dependent virus induction of the human IFN-β gene. *Cell*, **71**, 777–789.
57. Falvo,J.V., Thanos,D. and Maniatis,T. (1995) Reversal of intrinsic DNA bends in the IFN beta gene enhancer by transcription factors and the architectural protein HMG I(Y). *Cell*, **83**, 1101–1111.
58. Heyduk,E., Heyduk,T., Claus,P. and Wiśniewski,J.R. (1997) Conformational changes of DNA induced by binding of Chironomus high mobility group protein 1a (cHMG1a). Regions flanking an HMG1 box domain do not influence the bend angle of the DNA. *J. Biol. Chem.*, **272**, 19763–19770.
59. vanDuin,M., Koken,M.H., van den Tol,J., ten Dijke,P., Odijk,H., Westerveld,A., Bootsma,D. and Hoeijmakers,J.H. (1987) Genomic characterization of the human DNA excision repair gene ERCC-1. *Nucleic Acids Res.*, **15**, 9195–9213.
60. John,S., Reeves,R.B., Lin,J.X., Child,R., Leiden,J.M., Thompson,C.B. and Leonard,W.J. (1995) Regulation of cell-type-specific interleukin-2 receptor alpha-chain gene expression: potential role of physical interactions between Elf-1, HMG-I(Y) and NF-kappa B family proteins. *Mol. Cell Biol.*, **15**, 1786–1796.